NAL PROPOSAL No. 47

Correspondent: I. A. Pless
Lab for Nuclear Science
Mass. Inst. of Technology
Cambridge, Mass. 02139

FTS/Commercial 617-864-6900

DIFFRACTION DISSOCIATION AND ELASTIC SCATTERING PROCESSES WITH INCIDENT PROTONS AND NEGATIVE PIONS IN THE 200 GeV/c REGION

B. T. Feld, R. I. Hulsizer, V. Kistiakowsky, I. A. Pless
F. Triantis, J. Wolfson, R. K. Yamamoto

Massachusetts Institute of Technology

June 11, 1970

I COVER PAGE

TITLE AND ABSTRACT

"Diffraction Dissociation and Elastic Scattering Processes with Incident Protons and Negative Pions in the 200 GeV/c Region."

One purpose of this experiment is to measure the cross section for diffraction dissociation of target protons by 200 GeV/c incident protons and negative pions. Another purpose is to measure the elastic P-P and π-P cross section out to a $|t|$ of 2 $(GeV/c)^2$. In addition to the above measurements, the experiment can measure charged prong distributions, study single particle momentum distributions, and try to detect high mass resonances. The experiment utilizes a hybrid bubble chamber - wire chamber system. It will require 10^6 machine pulses equally divided between incident protons and pions. Part of the experiment is done with the information from both the bubble chamber and the wire chambers, while the large t elastic scattering data will be gathered using only the wire chambers with the bubble chamber serving as a hydrogen target. All data will be gathered during the same experimental run, a short pulse for the bubble chamber and a long spill for the elastic scattering large t measurement.

NAMES OF EXPERIMENTERS

B. T. Feld, R. I. Hulsizer, V. Kistiakowsky, I. A. Pless, F. Triantis, J. Wolfson and R. K. Yamamoto.

Date

11 June 1970

Name of Correspondent

I. A. Pless

II. PHYSICS JUSTIFICATION

A. Introduction:

Experiments at these (100-200 BeV) high energies present unique experimental problems, and there is little experience to build upon. However, there are at least two reactions for which one has a reasonable basis for making predictions.

The first is diffraction dissociation, the second, elastic scattering. Hence, this experiment proposes to study these two reactions in the 100-200 BeV range. The incident particles would be protons and π^- mesons. The detection apparatus would be a small bubble chamber preceded and followed by wire chambers and scintillation counters. The diffraction dissociation experiment would use the bubble chamber measurements plus the wire chamber information. The elastic scattering experiment would use the bubble chamber and wire chamber information for very small t. For large t, the bubble chamber would be used as a hydrogen target while the basic information would be gathered by the wire chambers and scintillation counters.

The t region spanned by the spectrometer alone would be $0.8 \leq |t| \leq 2.2$. This range would be covered without moving any of the beam line or spectrometer components.

The beam spill should have a short pulse containing an average of 4 particles which will be used for the bubble chamber. Following this there should be a long spill containing an average of 10^6 particles. This long spill will be used for the large t elastic scattering part of the experiment.

B. Theoretical And Experimental Background For Diffraction Dissociation

There seems to be no accepted definition for diffraction dissociation processes. In fact, a definitive description does not exist for any diffractive process. The following seem to be agreed on as general properties of diffraction dissociation.

1. The cross sections for such processes vary slowly with increasing bombarding energy.
2. No exchange of isotopic spin quantum numbers, strangeness and baryon number takes place.
3. The diffraction dissociated system is characterized by a low invariant mass.
4. The process occurs at small momentum transfers.
5. No G-parity exchange takes place.

The above properties are sometimes described as a Pomeranchuk exchange or a vacuum exchange. Such processes were first discussed explicitly (and named) by Good and Walker[1] in 1960. Since then they have been discussed by other authors, in particular Yang[2]. Yang characterizes these processes as those in which the target breaks up into n particles such that the total G, I^2, I^2_z and charge of these n particles equals that of the target.

Jackson[3] discusses the Pomeranchuk or vacuum trajectory as something special in the "hierarchy of Regge poles because (i) it is the highest lying trajectory, (ii) its slope seems abnormally small ($\alpha'_p \cong 0 - 0.3$ (BeV/c)^2), and (iii) there are serious doubts that it is a simple Regge pole. Some of the doubts concern the apparent slope and the lack of particles to associate with this trajectory; others stem

from a belief that diffractive scattering is a complicated shadowing effect, far more involved than the exchange of a single Regge pole."

The reactions that this experiment will explore are:

$$P+P \rightarrow (P\pi^0) + P \qquad (1)$$

$$P+P \rightarrow (N\pi^+) + P \qquad (2)$$

$$P+P \rightarrow (P\pi^+\pi^-) + P \qquad (3)$$

$$P+P \rightarrow (N\pi^+\pi^+\pi^-) + P \qquad (4)$$

$$\pi^-+P \rightarrow (P\pi^0) + \pi^- \qquad (5)$$

$$\pi^-+P \rightarrow (N\pi^+) + \pi^- \qquad (6)$$

$$\pi^-+P \rightarrow (P\pi^+\pi^-) + \pi^- \qquad (7)$$

$$\pi^-+P \rightarrow (N\pi^+\pi^+\pi^-) + \pi^- \qquad (8)$$

In the notation of Yang[2] the bracketed quantities form a $P^\dagger$. In these reactions the projectile (either proton or π^-) loses very little energy and leaves behing the $P^\dagger$. The prediction of Yang's theory is that these cross sections should remain constant or vary slowly with increasing energy of the projectile. Most of the other theories also imply a constant cross section as a function of energy for the above reactions. In particular, at high energies one expects that each of the above reactions will have a cross section which is a constant fraction of the elastic cross section.

There are experimental data on reactions (2) - (4). Figure 1 shows this evidence.[5] On this figure we have extrapolated the data to 500 GeV/c. If the cross sections continue in a general downward trend, all three of these cross sections will have a value of about 0.1 mb. at 200 GeV/c. However, if the cross sections have reached their limiting values at 30 GeV/c, then the cross sections will be about 1.0 mb. at 200 GeV/c. Isotopic spin considerations would lead to one half the above cross sections for reaction (1).

There is little experimental data on reactions (5) - (8). Since the πP elastic scattering cross section is approximately half that for PP elastic scattering, one would expect reactions (5) - (8) to have about half the cross sections of reactions (1) - (4). If these reactions are indeed related to a Pomeranchuk exchange, then one would also expect the corresponding channels to have the same properties regardless of whether or not a proton or pion initiated the event.

C. Theoretical And Experimental Background For Elastic Scattering

Much theoretical work has gone into the study of elastic proton-proton scattering and pion-proton scattering. Jackson [3] has given an excellent summary of current theoretical models to which we refer in all the following discussion. The main conclusion of this summary with respect to elastic scattering is that data are needed at higher energies.

Figure 2a contains data from Allaby et. al.[5] while figure 2b contains the data from Anderson et. al.[6] Interesting features of the data are the energy dependence at a fixed t, and the indication of a dip at $t \sim -1$ $(GeV/c)^2$. Figure 3a shows the comparison of the data of reference[6] with various models. The best fit seems to be the hybrid model of Chiu and Finkelstein.[7] This model is discussed in the summary by Jackson mentioned above. Figure 3b gives the predictions of this model for 25, 70 and 200 GeV/c; predictions this experiment will be able to test. The question of whether the π^- - P elastic peak does or does not shrink at this energy will be answered by this experiment. In any event, a study of elastic scattering out to a $|t|$ of 2 $(GeV/c)^2$ should help to differentiate among the various theoretical models and shed some light on the question of the Pomeranchuk limit.

D. By-Product Information

If the proposed experiments are successful, then there will be a considerable amount of additional information contained in the bubble chamber pictures and in the spark chamber records.

1. At the energies under study, it will be possible to obtain the distribution of multiplicity of charged particles in inelastic P-P and π-P interactions. Expectations are that this multiplicity should increase logarithmically with energy.

2. One of the most interesting possibilities will be that of comparing different theoretical approaches to the analysis of very high energy phenomena. For example, Feynman[10] treats specific reactions as involving either exchange or radiation of a spectrum of "partons" characterized, in the limit of infinite c.m. momentum, W, by the distribution dx/x, where $x = P_z/W$ is the center of mass longitudinal momentum of the product or products in question in units of W. In the Feynman approach, x and Q^2, the total transverse momentum, are the appropriate variables in terms of which a given set of reaction products should be analyzed.

Specific reactions are expected to exhibit Regge behavior, i.e., amplitudes proportional to $s^{\alpha(t)-1}$ where $\alpha(t)$ corresponds to the leading Regge trajectory.

Among the various specific reactions, only those represented by Pomeranchuk exchange, $\alpha(0) = 1$, (elastic scattering, diffraction dissociation) are expected to survive in the asymtotic limit $W \to \infty$. However, the residue of various inelastic reactions [whose number go to infinity as $W \to \infty$] should have a limiting single particle distribution in the

center of mass that is proportional to dx/x. This dx/x particle distribution can be looked for in the bubble chamber experiment.

3. The approach of Yang et. al.[2] is different. Considering essentially the diffraction dissociation reaction, they characterize the product distribution in terms of a fixed distribution of fragments resulting from the disruption of the target or the incident particle in question. The preferred system to analyze the target break up is the laboratory system, while the preferred system to analyze the projectile break up is the rest frame of the incoming particle.

This limiting fragmentation distribution for a given product is characterized by a momentum density, $P_i(\vec{p}_i)\, d^3 Pi$, which according to Yang's approach should become a constant at high energies. In this experiment, the slow particles in the bubble chamber should represent this limiting fragmentation of the target.

4. In addition to comparing the data to the theories of Feynman and Yang, one can examine the evidence for the existence of two body or quasi two body reactions. In general, if such reactions result from the exchange of any known particles [or Regge trajectories, excepting the Pomeranchuk], the individual cross sections are expected to fall off rapidly, as some power of the incident momentum. Nevertheless, it will be interesting to look for evidences of these reactions, especially of those reactions that might contain new resonances of higher mass than those already known. In this regard, the techniques of multi-dimensional prism-plot analysis, developed in this laboratory for multi-body final states, should prove very useful at the higher energies. Since all events will be measured, it will be simple to make the analysis.

III. EXPERIMENTAL ARRANGEMENT

A. Equipment And Set Up

This experiment will require the use of a hybrid system consisting of a small bubble chamber, wire spark chambers and scintillation counters. This system should be installed in the high resolution high momentum beam. Figure 4 is a schematic of the setup.

The incoming beam is defined by the scintillation counter C and small wire planes 1, 2, 3, 4. The fast outgoing particle is analyzed by the wire planes 9, 10, 11. 12. The geometry is chosen for incident particles of 200 GeV. For lower energy, one might alter some of the dimensions slightly. The $|t|$ range covered is from 0-2 $(BeV/c)^2$.

The wire chambers immediately following the bubble chamber are best viewed as extensions of the bubble chamber itself. They, plus the fringing field of the magnet, allow a much more precise measurement of the fast outgoing particles than can be achieved using the bubble chamber alone.

During the long beam spill, the bubble chamber will be used as a hydrogen target, and the wire chambers and deflecting magnets will act as a single arm spectrometer to measure the large t elastic scattering cross section. The counter hodoscope will allow triggering the wire chambers on preselected $|t|$ intervals during this part of the experiment. The t range can be covered by this equipment without moving any of the components in the beam line or experimental set up.

There should be a short beam spill for the bubble chamber followed by a long spill for the large t elastic scattering part of the experiment. The short spill should contain an average of 4 particles and the long spill, an average of 10^6 particles.

The deflection magnets might be similar to the ANL BM 105 design. This design is included in the appendix.

The wire chambers A, B, C, D, shown above and below the bubble chamber would be useful in this experiment, but are not crucial, and their existence has not been assumed in any calculation. They are discussed in Section IV, as is the bubble chamber itself.

B. Data Analysis

This experiment will require 1 million pulses of the machine, five hundred thousand with incident protons and five hundred thousand with incident π^-. Table IA shows the expected yield for the bubble chamber part of the experiment, and table IB shows the expected yield of the large t elastic scattering part of the experiment.

There are a few assumptions that go into table I. The first is that the machine will operate first with a short spill for the bubble chamber (average of four tracks per short spill), followed by a long spill (average 10^6 particles per long spill) for the portion of the experiment that uses the bubble chamber simply as a hydrogen target.

The second is that the spot size of the beam will be about 4 centimeters in diameter, and the divergence will be ± 1 milliradian at the hydrogen target (bubble chamber). Another assumption is the cross sections listed. These come from the hybrid model[7] and from the Orear parameterization.[8]

The yields listed in table I depend somewhat on the exact bubble chamber chosen. In the case of the large t elastic scattering part of the experiment, the yields will depend on the amount of background in the experimental hall and the nature of the competing high energy processes.

The main purpose of table I is to indicate the possible statistics available to this experiment and are only accurate to about a factor of 2.

An important part of the analysis of the bubble chamber data is the separation of the eight channels we are interested in from all other reactions. The most difficult separations come in the following cases:

a) $P+P \rightarrow (P\pi^0)+P$ versus ā) $P+P \rightarrow P+P+\pi^0+\pi^0$

b) $\pi^-+P \rightarrow (P\pi^0)+\pi^-$ versus b̄) $\pi^-+P \rightarrow P+\pi^-+\pi^0+\pi^0$

c) $P+P \rightarrow (N\pi^+)+P$ versus c̄) $P+P \rightarrow N+P+\pi^+ +\pi^0$

d) $\pi^-+P \rightarrow (N\pi^+)^+\pi^-$ versus d̄) $\pi^-+P \rightarrow N+\pi^-+\pi^+ +\pi^0$

All other reactions are four constraint reactions, and there is less difficulty with them. For the reaction a) versus ā) we assumed that the $(P\pi^0)$ had an invariant mass centered at 1400 MeV with a width of 400 MeV. For the $P+\pi^0+\pi^0$ we assumed an invariant mass centered at 2400 MeV with a width of 2200 MeV. In both cases we used a production distribution of e^{10t} and isotropic decay. Putting in realistic bubble chamber measuring errors [taken from our experience with the ANL 30" chamber] and known properties of wire chambers,[9] we performed a Monte Carlo calculation to determine the separation.

The result is that the two processes separate with a maximum contamination of less than 10%. We checked the contamination of the elastic scattering in this channel due to measurement errors. We took into account the 12 times larger cross section for the elastic channel. Again, the processes separate with less than 10% of the events $(P\pi^0)+P$ being contaminated by misidentified elastic events. All calculations were made at 200 GeV/c.

Similar calculations were made for channel b, b̄; c, c̄; and d, d̄; with the same result. The separation can be made at these energies.

This separation depends upon which bubble chamber one uses. As noted, we used the properties of the ANL 30" bubble chamber.

For the large t elastic scattering part of the experiment, we use the system as a single arm spectrometer. The incident and the fast outgoing particle are measured, both in angle and momentum. Hence, for this part of the experiment, this is a missing mass spectrometer. Again, the main difficulty is separating the elastic scattering from the production of one pion, i.e., from the diffraction dissociation. This also has been tested with a Monte Carlo calculation, and we find a good separation out to a $|t|$ of 2 $(GeV/c)^2$. Out to this t, there is less than 2% contamination of the elastic by the diffraction dissociation. There is no confusion between elastic scattering and the reaction $P+P \rightarrow P+N+\pi^+$.

The gathering of the data will be done with the aid of a small computer (PDP-9 class). All data will be recorded on magnetic tape. The computer will be used to spot check part of the experiment in real time, but the main data reduction will be off line. In addition, the particles that pass through the equipment without interacting will be used as a continual check on the alignment of the chambers. The scintillation hodoscope will be particularly useful for this. In addition, one will periodically use the wire chambers themselves to test alignment.

We will use PEPR to measure the events in the bubble chamber film. PEPR will also correlate the information from the wire chambers so that the complete information will be passed onto subsequent analysis programs. When fully staffed, the PEPR group can handle 10^6 events per year. The intention is to measure all events, not just elastic scattering and diffraction dissociation. Hence, we will get an all-over view of what the situation is in these high energy collisions.

B. Testing And Data Accumulation Time

The time required for setting up and testing the bubble chamber depends on which chamber is chosen and the staff available to do the job. However, most, if not all the installation and testing could occur before beam time, if an early decision is made.

The testing time for the wire chambers and debugging the data gathering and display programs could be done in two months. However, the question of strong radiation and experimental hall background could make this estimate optimistic. Moreover, the installation of the chambers depends on availability of on-site facilities, such as portable buildings, roads, etc. Here again, a lot of installation could take place before beam time if decisions are made early enough.

We should emphasize, that the proposed set up is an initial design. Undoubtedly, some changes will be made to make installation simpler, depending on site situation. We will be continually improving the designs of the set up as beam design and other factors become better known. For example, the 100 meter lever arm could be shortened with a small sacrifice in resolution. A more important fact will be the actual energy used in the experiment. If the energy is 160 GeV/c, some of the design problems will be easier, and some will be harder. Also exactly which magnets are used in the deflecting system will play a strong role in determining the final system.

The data accumulation time if 10^6 useful pulses of the accelerator; 5×10^5 with protons and 5×10^5 with negative mesons. A useful pulse is defined as a short pulse with an average of 4 particles and a long pulse with an average of 10^6 particles.

IV. APPARATUS

There are at least 5 small bubble chambers that would be suitable for this experiment.

These are:

1. 40" - SLAC
2. 30" - ANL
3. 500 liter - ANL
4. 30" - BNL
5. 31" - BNL

Any of these chambers are suitable for this experiment. However, one must be certain that the chosen chamber has both thin entrance and exit windows. For some of the above chambers [i.e., 40" SLAC; 500 Liter ANL] one can place wire chambers either above or below the bubble chamber. These are shown as AB and CD in figure 4. These wire chambers would be useful in this experiment but are not crucial. Their existence was not assumed in any of the above calculations.

The members of this experimental group are prepared to aid in the acquisition of such a bubble chamber, its installation and initial operation at NAL. We are aware that bringing an existing chamber to NAL for a physics program will require extensive negotiations between NAL, various other national laboratories and the rest of the physics community. If NAL determines that a small chamber is desirable for its physics program and decides on the bubble chamber it considers best for this purpose, then the members of this experimental group will join other interested parties to aid in the negotiations to bring that chamber to NAL under conditions thought appropriate by NAL.

The other pieces of equipment that this experiment requires are the four deflecting magnets. These could be the same design as the ANL BM(105). This

design is in Appendix 3. It would be desirable if these, or similar magnets were part of the NAL experimental equipment pool. However, the spectrometer probably could be redesigned about any standard magnets.

The funding at LNS-M.I.T. for the next few years is uncertain, but within the limits of fiscal responsibility, it is expected that M.I.T. would furnish the wire chambers, counters, and on-line computer [PDP-9 class].

It is our opinion that the small bubble chamber could be in operation within 18 months after the device is on the NAL site. The rest of the equipment for this experiment could easily match this, or shorter, time scale.

TABLE I A (Bubble Chamber)

Reaction	Assumed σ Total	Yield
$P+P \rightarrow (P\pi^0)+P$	1.0 mb	5,000
	0.1 mb	500
$P+P \rightarrow (N\pi^+)+P$	1.0 mb	10,000
	0.1 mb	1,000
$P+P \rightarrow (P\pi^+\pi^-)+P$	1.0 mb	10,000
	0.1 mb	1,000
$P+P \rightarrow (PN\pi^+\pi^+\pi^-)+P$	1.0 mb	10,000
	0.1 mb	1,000
$P+P \rightarrow P+P$	12 mb	130,000
$\pi^-+P \rightarrow (P\pi^0)+P$	0.5	2,500
	.05	250
$\pi^-+P \rightarrow (N\pi^+)+P$	0.5	5,000
	.05	500
$\pi^-+P (P\pi^+\pi^-)+P$	0.5	5,000
	.05	500
$\pi^-+P (PN\pi^+\pi^+\pi^-)+P$	0.5	5,000
	.05	500
$\pi^-+P \rightarrow \pi^-+P$	6 m 6	65,000

TABLE I B (Large t Elastic Scattering)

Reaction	$\|t\|$ range	σ	Yield
$P+P \rightarrow P+P$	1.0 - 1.2	9×10^{-31}	90,000
	1.2 - 1.4	1×10^{-31}	10,000
	1.4 - 1.6	0.5×10^{-31}	5,000
	1.6 - 1.8	0.5×10^{-31}	5,000
	1.8 - 2.0	0.5×10^{-31}	5,000
	2.0 - 2.1	0.5×10^{-31}	5,000
	2.1 - 2.2	0.5×10^{-31}	5,000
$\pi^- + P \rightarrow \pi^- + P$	1.0 - 1.2	5.0×10^{-30}	200,000
	1.2 - 1.4	1.0×10^{-30}	40,000
	1.6 → 1.8	0.5×10^{-30}	20,000
	1.8 → 2.0	1×10^{-31}	10,000
	2.0 → 2.1	0.5×10^{-31}	5,000
	2.1 → 2.2	0.5×10^{-31}	5,000

Table I assumes that the experiment will consist of 500,000 pulses with incident protons and 500,000 pulses with incident pions.

APPENDIXES

1. Reprint from Physical Review 188, 5, 2159, Dec. 25, 1969
   " Hypothesis of Limiting Fragmentation in High-Energy Collisions",
   J. Benecke, T. Chou, C. Yang, and E. Yen.

2. Preprint.
   " The Behavior of Hadron Collisions at Extreme Energies "
   Richard P. Feynman, Calif. Institute of Tech, Oct. 1969

3. Excerpt from 3/69 Issue of Users Handbook -- Argonne National Laboratory
   Page 5.7 A: 18 VI 72 (BM) 105) Bending Magnet

Figure 1

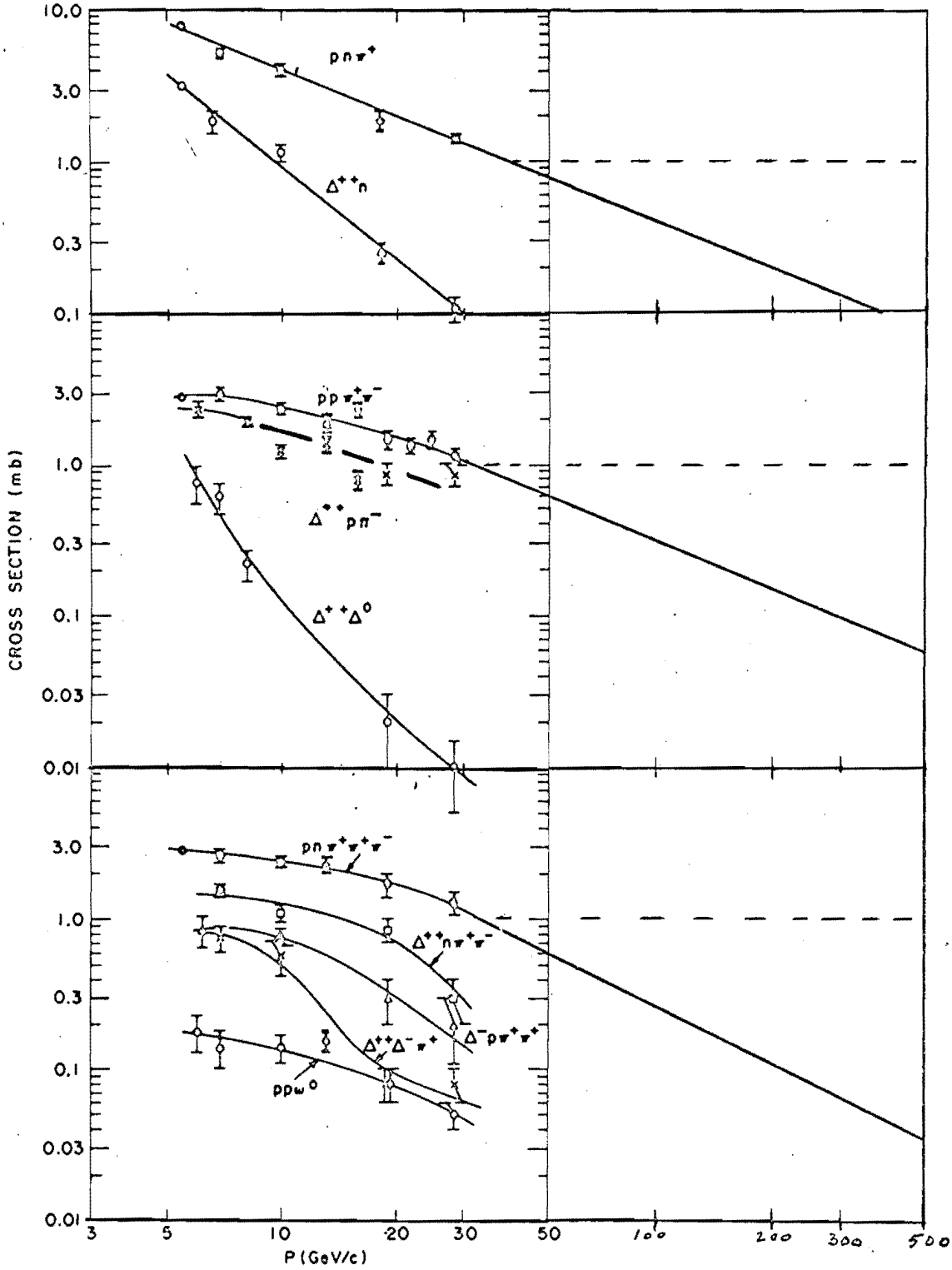

Cross-section for the production of various final states in the reactions $pp \to pn\pi^+$ (top), $pp \to pp\pi^+\pi^-$ (middle) and $pp \to$ $\to pn\pi^+\pi^+\pi^-$ (bottom) as a function of incident laboratory momentum.

Solid and dashed lines are possible extrapolations to high energy.

Figure 2

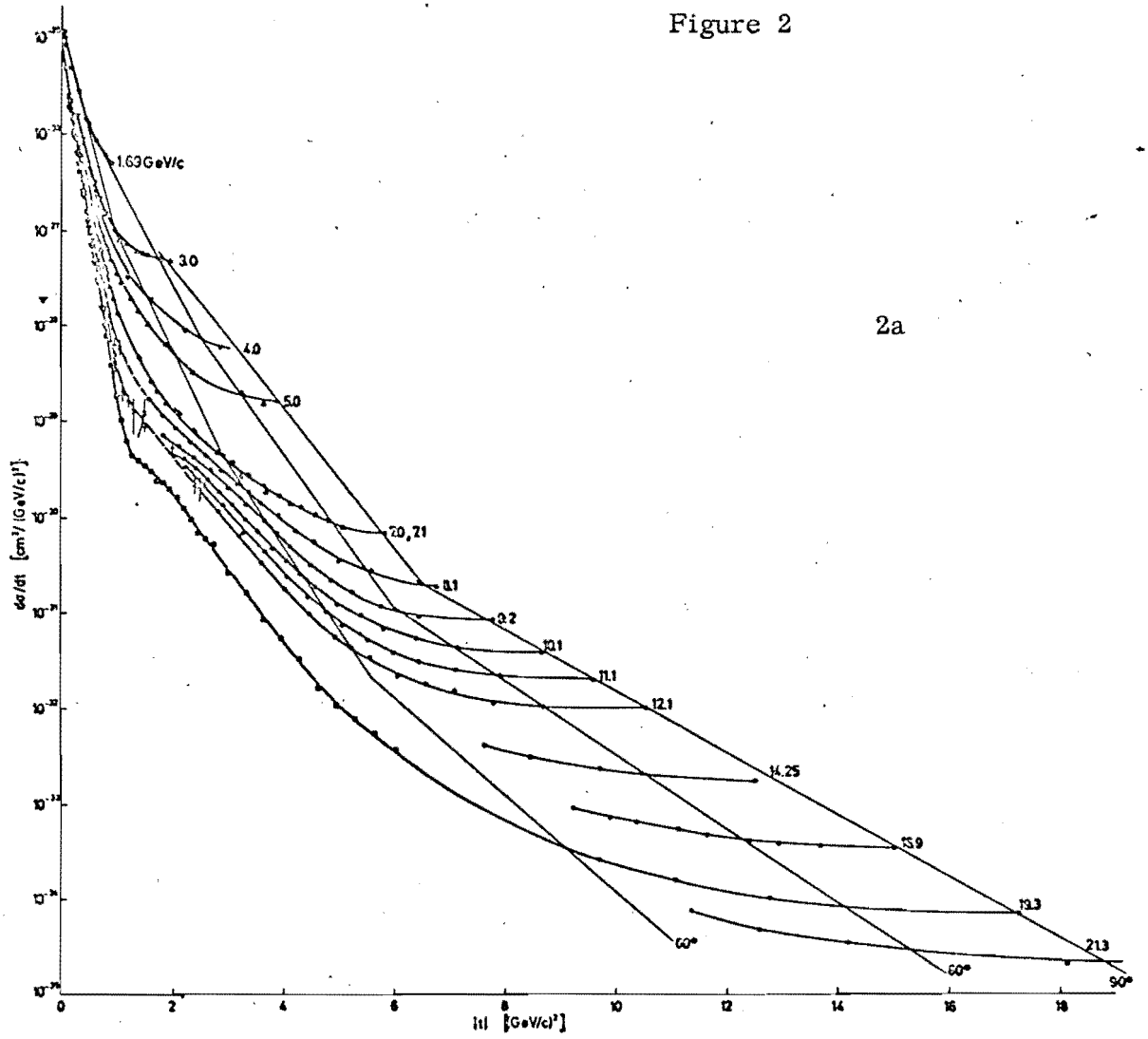

2a

Differential cross section for *pp* elastic scattering at 19.2 GeV/c, along with results at other incident momenta

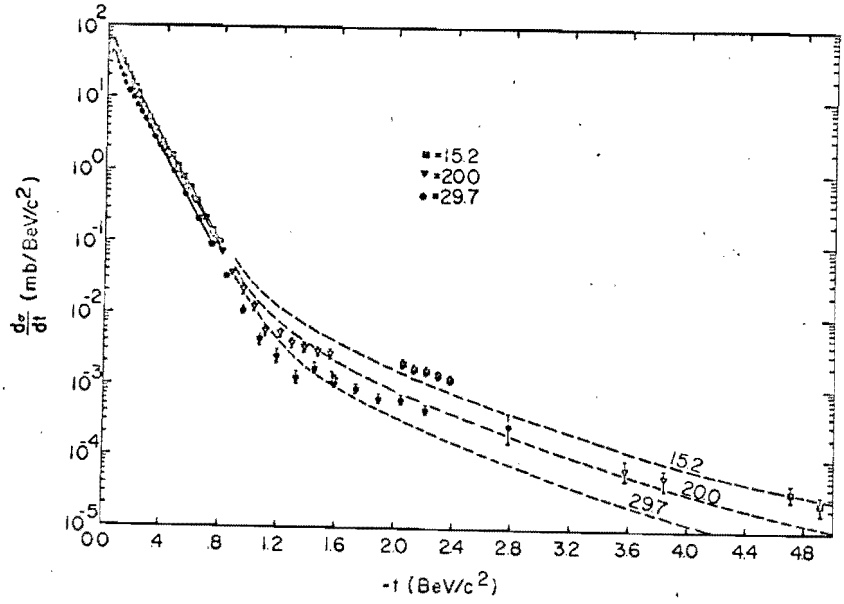

2b

p–p elastic cross section

Figure 3

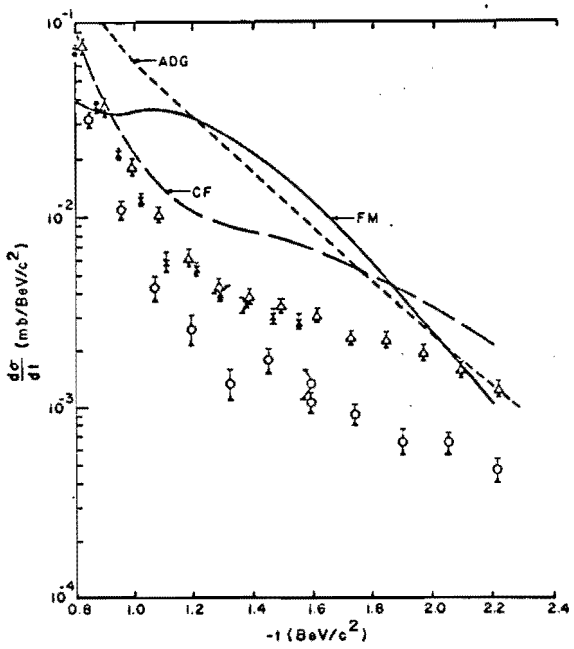

3a

p-p elastic cross section as a function of t in the region of $|t| = 1.0$ (BeV/c)^2. Circles are the 29.74-BeV/c points, crosses are the 20.0-BeV/c points. Triangles are the data of Allaby et al. at 19.2 BeV/c. The solid line is the 30-BeV/c prediction of Frautschi and Margolis. The short-dashed line is the asymptotic cross section of Abarbanel, Drell, and Gilman . The long-dashed line is the 25-BeV/c cross section of Chiu and Finkelstein. [Note that the y axis is at $-t = 0.8$ (BeV/c)^2, not at $t = 0.0$ (BeV/c)^2.]

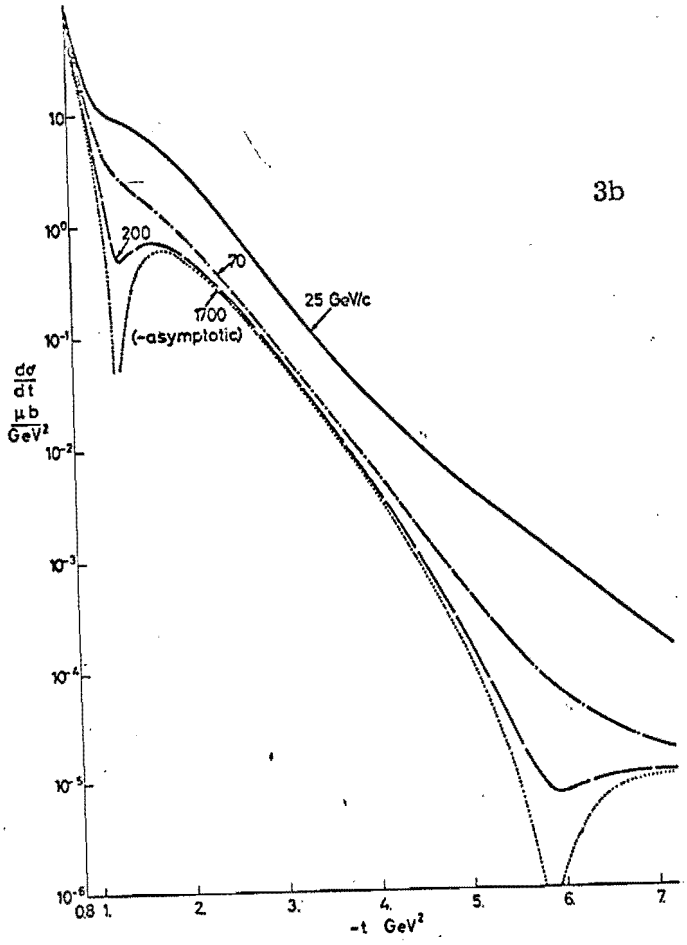

3b

Differential cross section for pp scattering predicted by the hybrid model at various incident momenta (from Chiu and Finkelstein)

Figure 4

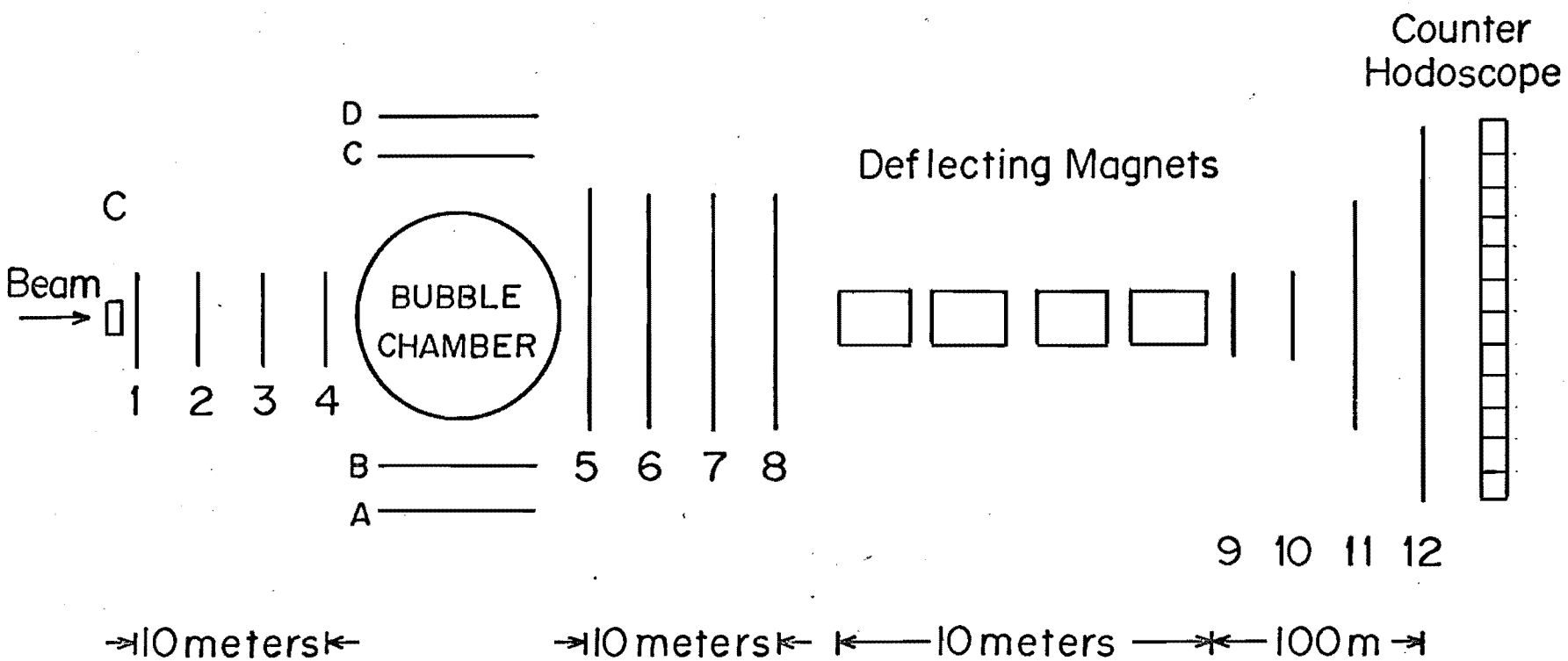
Counter
Hodoscope
D
C
Deflecting Magnets
C
Beam
BUBBLE
CHAMBER
1 2 3 4
B
A
5 6 7 8
9 10 11 12
10 meters
10 meters
10 meters
100 m
(not to scale)